Toxicology in Vitro 58 (2019) 195–206

Contents lists available at ScienceDirect

Toxicology in Vitro

journal homepage: www.elsevier.com/locate/toxinvit

Basal but divergent: Clinical implications of differential coagulotoxicity in a clade of Asian vipers

Jordan Debono[a], Mettine H.A. Bos[b], Francisco Coimbra[a], Lilin Ge[c,d], Nathaniel Frank[e], Hang Fai Kwok[c,*], Bryan G. Fry[a,*]

[a] Venom Evolution Lab, School of Biological Sciences, University of Queensland, St Lucia, QLD 4072, Australia
[b] Division of Thrombosis and Hemostasis, Einthoven Laboratory for Vascular and Regenerative Medicine, Leiden University Medical Center, Albinusdreef 2, 2333 ZA, Leiden, the Netherlands
[c] Institute of Translational Medicine, Faculty of Health Sciences, University of Macau, Avenida da Universidade, Taipa, Macau
[d] State Key Laboratory Cultivation Base for TCM Quality and Efficacy, School of Pharmacy, Nanjing University of Chinese Medicine, 138 Xianlin Avenue, Qixia District, Nanjing 210046, China
[e] Mtoxins, 1111 Washington Ave, Oshkosh, WI 54901, USA

A B S T R A C T

Envenomations by Asian pitvipers can induce multiple clinical complications resulting from coagulopathic and neuropathic effects. While intense research has been undertaken for some species, functional coagulopathic effects have been neglected. As these species' venoms affect the blood coagulation cascade we investigated their effects upon the human clotting cascade using venoms of species from the *Azemiops, Calloselasma, Deinagkistrodon* and *Hypnale* genera. *Calloselasma rhodostoma, Deinagkistrodon acutus,* and *Hypnale hypnale* produced net anticoagulant effects through pseudo-procoagulant clotting of fibrinogen, resulting in weak, unstable, transient fibrin clots. *Tropidolaemus wagleri* was only weakly pseudo-procoagulant, clotting fibrinogen with only a negligible net anticoagulant effect. *Azemiops feae* and *Tropidolaemus subannulatus* did not affect clotting. This is the first study to examine in a phylogenetic context the coagulotoxic effects of related genera of basal Asiatic pit-vipers. The results reveal substantial variation between sister genera, providing crucial information about clinical effects and implications for antivenom cross-reactivity.

1. Introduction

Snakebite is one of the most neglected tropical diseases worldwide (Fry, 2018; Gutiérrez et al., 2006; Williams et al., 2010; Williams et al., 2011). Human-snake conflicts are increasing due to a myriad of factors including human population expansion and increase in snake activity periods due to climate change (Fry, 2018). Consequently a need for a better understanding into the effects of envenomations in humans is required. Snakebite is considered a current global health crisis, however it has been neglected, ignored, underestimated and misunderstood despite its ever-increasing significance (Fry, 2018). Additionally, there is lack of appropriate medical treatment and assistance to those who are affected by snakebite due to several contributing factors including education, financial aid and proximity to health care facilities. Many people who are envenomated and survive are left with permanent disabilities and crippling medical bills, even if medical treatment is sought out. Although antivenoms do exist for some species, many species of venomous snakes do not have an appropriate antivenom available or it is far too expensive for patients to purchase. Snakebite however is not restricted to the poorer regions of the world and many exotic venomous snake species kept in private collections can inflict potentially fatal envenomations, which is only potentiated by unsupported questionable alternative first aid treatments that are being supplied (Fry, 2018).

Snake venom is made up of a myriad of toxins which can deleteriously affect any part of haemostasis, resulting in an array of variable outcomes. In humans this can range from localised tissue swelling and damage, to necrosis, respiratory failure, renal failure, kidney failure and haemorrhagic shock (Alirol et al., 2010; Ariaratnam et al., 2008; Dharmaratne and Gunawardena, 1988; Fry, 2018; Oulion et al., 2018; Sutherland, 1983; Tan and Tan, 1989; Tang et al., 2016; White, 2005). Venoms that affect coagulation do so via various coagulotoxic mechanisms ranging from procoagulant through to strong anticoagulant activities, through the disruption of clotting enzymes (Fry et al., 2009). Procoagulant snake venoms produce endogenous thrombin through the activation of Factor X or prothrombin, resulting in strong, stable fibrin clots (which are further stabilised by the endogenous thrombin activating Factor XIII) while anticoagulant venoms effect upon fibrinogen is either through destructive cleavage of fibrinogen or the pseudo-procoagulant mechanism of cleaving fibrinogen to form abnormal, short-

* Corresponding authors.
E-mail addresses: hfkwok@um.edu.mo (H.F. Kwok), bgfry@uq.edu.au (B.G. Fry).

https://doi.org/10.1016/j.tiv.2019.03.038
Received 14 March 2019; Received in revised form 27 March 2019; Accepted 27 March 2019
Available online 28 March 2019
0887-2333/ © 2019 Elsevier Ltd. All rights reserved.

lived fibrin clots (thus having a net anticoagulant effect), (Dambisya et al., 1994; Debono et al., 2018; Fry et al., 2009; Isbister, 2009).

The Viperidae snake family mainly affect the blood coagulation system and are responsible for a large proportion of global snake bites. Vipers inhabit Africa, the Americas, Asia, and Europe Viperidae is split into three sub families; Crotalinae (pit vipers), Viperinae (true vipers) and Azemiopinae (Alencar et al., 2018; Alencar et al., 2016). This split occurred approximately 50 million years ago (MYA) and Crotaline has been under immense diversification and expansion for the past 41 MYA (Alencar et al., 2018; Alencar et al., 2016). Crotalinae occupy a large geographical range, from most of Asia throughout all of the Americas, and includes genera such as, *Bothrops, Crotalus,* and *Trimeresurus*. In Asia, a basal clade consists of the morphologically similar terrestrial genera, *Calloselasma*, *Deinagkistrodon*, and *Hypnale* along with the highly derived arboreal genus *Tropidolaemus* (Alencar et al., 2018). As this clade is a mixture of terrestrial and arboreal species and therefore provides an excellent opportunity to investigate venom adaptive evolution. The highly derived genus semi-fossorial genus *Azemiops* provides a further point of comparison.

Asian viper venoms are well known for effects on bite victims including haemorrhagic shock, necrosis and thrombocytopenia, spontaneous haemorrhage and acute kidney injury (Ariaratnam et al., 2008; de Silva et al., 1994; Herath et al., 2012; Joseph et al., 2007; Maduwage et al., 2013a; Maduwage et al., 2013b; Tang et al., 2016; Weerakkody et al., 2016; Withana et al., 2014). Haemorrhagic effects are potentiated by fibrinogenolytic enzymes which may act upon fibrinogen to either directly produce anticoagulation, by destructively cleave fibrinogen, or to indirectly produce anticoagulation by cleaving fibrinogen to form short-lived, weak clots in a pseudo-procoagulant manner (Coimbra et al., 2018; Debono et al., 2018; Dobson et al., 2018; Esnouf and Tunnah, 1967; Huang et al., 1992; Levy and Del Zoppo, 2006; Nielsen, 2016b; Premawardena et al., 1998; Trookman et al., 2009; Zulys et al., 1989).

There are significant variations in the venoms of this clade which have accumulated during long periods of evolutionary divergence contributing to variable antivenom efficacy (Ali et al., 2013; Daltry et al., 1996; Mebs et al., 1994; Tan et al., 2017; Tang et al., 2016). Previous studies have shown that some species affect various sites along the cascade such as platelet activity (Kong and Chung, 2001; Navdaev et al., 2011; Shin and Morita, 1998; Wang et al., 1999), FX activation and prothrombin activation (Ainsworth et al., 2018; Leong et al., 2014; Yamada et al., 1997).

The inter-genus venom variation between Asian pit vipers is unknown and some lineages have been left completely unstudied. As a result, there is limited knowledge about their effects on coagulation of the human body. Here we investigate the relationship and mechanisms behind their coagulotoxicity and illustrate the variations within the basal Asian pit vipers genera *Azemiops, Calloselasma*, *Deinagkistrodon*, *Hypnale*, and *Tropidolaemus*. By contributing to the broader understanding of venom functional variation, improvement in clinical management strategies may be developed, as well as the potential for discovery of novel compounds useful in the advancement of blood clotting disorder therapeutics and diagnostics surrounding thrombosis and haemostasis.

2. Materials and methods

2.1. Venoms

Six species of Asian Viperidae (Alencar et al., 2016) were investigated for venom composition and coagulation effects via a multidisciplinary approach of venomics, functionality and bioactivity. Pooled, lyophilized venom samples from species *Azemiops feae, Calloselasma rhodostoma*, *Deinagkistrodon acutus*, *Hypnale hypnale*, *Tropidolaemus subannulatus* and *Tropidolaemus wagleri* were procured from captive collections (unknown localities of founding stocks). Venoms were resuspended in deionized H_20 and protein concentrations (mg/ml) determined using a ThermoFisher Scientific Nanodrop™ 2000c Spectrophotometer. Working stocks of 50% deionized water/50% glycerol (> 99%, Sigma-Aldrich) for all venoms were prepared at 1 mg/ml and stored at −20 °C to preserve enzymatic activity and reduce enzyme degradation. Venoms included in the following assays were subject to availability at the time of analysis.

2.2. Enzyme assays

Various enzymatic assays were performed to investigate activity on specific artificial substrates, as well as PLA_2, plasminogen activation, prothrombin activation and FX activation. Investigation followed that described by (Debono et al., 2018). Phytools heat mapping followed that of (Lister et al., 2017). Details are as follows.

2.2.1. Fluorescent substrate activation

In order to investigate Fluorescent Determination of matrix metalloprotease (ES001, ES003, ES005, ES010), serine protease activity (ES002, ES011) and phospholipase A_2 (PLA_2) enzymatic assays were undertaken as previously described by us (Debono et al., 2017a). For matrix metalloprotease and serine protease assays a working stock solution of freeze dried venom was reconstituted in a buffer containing 50% MilliQ/50% glycerol (> 99.9%, Sigma, St Louis, MO, USA) at a 1:1 ratio to preserve enzymatic activity and reduce enzyme degradation. Varying concentrations of crude venom (10 ng/μl and 50 ng/μl) were plated out in triplicates on a 384-well plate (black, Lot#1171125, nunc™ Thermo Scientific, Rochester, NY, USA) and measured by adding 90 μl quenched fluorescent substrate per well (total volume 100 μl/well, 10 μl/5 ml enzyme buffer, 150 mM NaCl, and 50 mM Tri-HCl (pH 7.3), Fluorogenic Peptide Substrate, R & D systems, Cat#ES001, ES003, ES005, ES010, ES011, Minneapolis, Minnesota). Fluorescence was monitored by a Fluoroskan Ascent™ (Thermo Scientific, Vantaa, Finland) Microplate Fluorometer (Cat#1506450, Thermo Scientific, Vantaa, Finland) (Cat#ES001, ES003, ES005, ES010 for Matrix Metalloprotease at an excitation of 320 nm, emission at 405 nm; Cat#ES011 for Kallikrein at an excitation of 390 nm, emission at 460 nm) over 400 mins or until activity had ceased. Data was collected using Ascent® Software v2.6 (Thermo Scientific, Vantaa, Finland).

For PLA_2 analysis we assessed the continuous Phospholipase A_2 (PLA_2) activity of the venoms using a fluorescence substrate assay (EnzChek® Phospholipase A_2 Assay Kit, Cat#E10217, Thermo Scientific, Rochester, NY, USA), measured on a Fluoroskan Ascent® Microplate Fluorometer (Cat#1506450, Thermo Scientific, Vantaa, Finland). As above, we used a working stock solution of freeze dried venom reconstituted in a buffer containing 50% MilliQ/50% glycerol (> 99.9%, Sigma) at a 1:1 ratio. A concentration of enzyme activity in venom (50 ng/μl) was brought up in 12.5 μl 1× PLA_2 reaction buffer (50 mM Tris-HCL, 100 mM NaCl, 1 mM $CaCl_2$, pH 8.9) and plated out in triplicates on a 384-well plate (black, Lot#1171125, nunc™ Thermo Scientific, Rochester, NY, USA). The triplicates were measured by dispensing 12.5 μl quenched 1 mM EnzChek® (Thermo Scientific, Rochester, NY, USA) Phospholipase A_2 Substrate per well (total volume 25 μl/well) over 100 min or until activity had ceased (at an excitation of 485 nm, emission 538 nm). Purified PLA_2 from bee venom (1 U/ml) was used as a positive control and data was collected using Ascent® Software v2.6 (Thermo Scientific, Vantaa, Finland).

2.2.2. Plasminogen activation

The same working stock solution of 1 mg/ml (outlined above and in (Debono et al., 2017a) of freeze dried venom was used to make the following dilutions: 10 ng/μl, 50 ng/μl and 100 ng/μl. These varying concentrations of enzyme activity in venom were plated out on a 384-well plate (black, Lot#1171125, nunc™ Thermo Scientific, Rochester, NY, USA) in triplicates, with and without 10 ng/μl plasminogen per well (Lot#FF0125 HCPG-0130, Haematologic Technologies Inc., Essex

Junction, VT, USA). Plasminogen, a serine protease, can be activated by a serine protease specific substrate (Fluorogenic Peptide Substrate, R & D systems, Cat# ES011, Minneapolis, Minnesota). Plasmin was used as a positive control (10 ng/μl per positive control well, Lot#EE1120, HCPM-0140, Haematologic Technologies Inc., Essex Junction, VT, USA). Activation from venoms was measured by adding 90 μl quenched fluorescent substrate per well (total volume 100 μl/well; 20 μl/5 ml enzyme buffer - 150 mM NaCl and 50 mM Tri-HCl (pH 7.3), Fluorogenic Peptide Substrate, R & D systems, Cat#ES011, Minneapolis, Minnesota). Fluorescence was monitored by a Fluoroskan Ascent™ Microplate Fluorometer (Cat#1506450, Thermo Scientific, Vantaa, Finland) at excitation 390 nm and emission at 460 nm over 150mins or until activity had ceased. Data was collected using Ascent® Software v2.6 (Thermo Scientific, Vantaa, Finland). Experiments were conducted in triplicate.

2.2.3. Prothrombin activation

The ability for the above crude venom to directly activate prothrombin was investigated and measured by modifying the above protocol used for plasminogen activation. Plasminogen was replaced with prothrombin (Lot#EE0930, HCP-0010, Haematologic Technologies Inc., Essex Junction, VT, USA) and plasmin was replaced with thrombin (Lot#FF0315, HCT-0020, Haematologic Technologies Inc., Essex Junction, VT, USA) as a positive control (10 ng/μl per positive control well). Data was collected using Ascent® Software v2.6 (Thermo Scientific, Vantaa, Finland). Experiments were conducted in triplicate.

2.2.4. Factor X activation

The ability for the above crude venom to directly activate blood coagulation Factor X (FX) was investigated and measured by modifying the above protocol used for plasminogen activation using FX (Lot#FF0407, HCX-0050, Haematologic Technologies Inc., Essex Junction, VT, USA) as the experimental target and FXa (Lot#EE1102, HCXA-0060, Haematologic Technologies Inc., Essex Junction, VT, USA) as the positive control (10 ng/μl per positive control well). Data was collected using Ascent® Software v2.6 (Thermo Scientific, Vantaa, Finland). Experiments were conducted in triplicate.

2.2.5. Phylogenetic comparative analyses

Observed venom activities of the different snake species were investigated in an evolutionary framework by mapping them on a taxon tree using Mestique and analyses were performed via the R package Phytools as per that of (Lister et al., 2017; Rogalski et al., 2017) using phylogenetic Generalized Least Squares (PGLS). The phylogeny was adapted from (Alencar et al., 2016) Analyses were implemented in R v3.2.5 (Team, 2016) using the APE package for basic data manipulation (Paradis et al., 2004). Ancestral states of each substrate functional trait (ES001, ES002, ES003, ES005, ES010, ES011, PLA_2, coagulation) were estimated via maximum likelihood with the contMap function in phytools (Revell, 2012).

2.3. Coagulation assays

Action upon plasma and fibrinogen:

2.3.1. Clot formation or inhibition assays

Ability to affect clotting of plasma and fibrinogen, including relative co-factor dependency, was investigated using a Stago STA-R Max coagulation analyser using protocols previously described by us (Debono et al., 2018; Debono et al., 2017a). Details are as follows.

In order to investigate whole plasma and fibrinogen clotting and co-factor dependency clotting, we prepared healthy human plasma (citrate 3.2%, Lot#1690252, approval #16-04QLD-10), obtained from the Australian Red Cross (44 Musk Street, Kelvin Grove, Queensland 4059) and human fibrinogen (4 mg/ml, Lot#F3879, Sigma Aldrich, St. Louis, Missouri, United States). Coagulopathic toxin effects were measured by a modified procoagulant protocol on a Stago STA-R Max coagulation robot (France) using Stago Analyser software v0.00.04 (Stago, Asniéres sur Seine, France). Plasma clotting baseline parameters were determined by performing the standardised activated Partial Thromboplastin Time (aPTT) test (Stago Cat# T1203 TriniCLOT APTT HS). This was used as a control to determine the health of normal clotting plasma according to the universal standard range of between 27 and 35 s. Plasma aliquots of 2 ml, which had been flash frozen in liquid nitrogen and stored in a − 80 °C freezer, were defrosted in an Arctic refrigerated circulator SC150-A40 at 37 °C. In order to determine clotting times effected by the addition of varying venom concentrations, a modified aPTT test was developed. A starting volume of 50 μl of crude venom (5 μg/50 μl) was diluted with STA Owren Koller Buffer (Stago Cat# 00360). An 8-dilution series of 1 (20 μg/ml), 1/2 (10 μg/ml), 1/5 (4 μg/ml), 1/12 (1.6 μg/ml), 1/30 (0.66 μg/ml), 1/80 (0.25 μg/ml), 1/160 (0.125 μg/ml), and 1/400 (0.05 μg/ml) was performed in triplicate. $CaCl_2$ (50 μl; 25 mM stock solution Stago Cat# 00367 STA $CaCl_2$ 0.025 M) was added with 50 μl phospholipid (solubilized in Owren Koller Buffer adapted from STA C·K Prest standard kit, Stago Cat# 00597). An additional 25 μl of Owren Koller Buffer was added to the cuvette and incubated for 120 s at 37 °C before adding 75 μl of human plasma. Relative clotting was then monitored for 999 s or until plasma clotted (whichever was sooner). Additional tests were run, both with and without $CaCl_2$ and phospholipid, respectively, to test for $CaCl_2$ or phospholipid dependency. STA Owren Koller Buffer was used as a substitute, using the same volumes to allow for consistency in the final volumes (250 μl).

2.3.2. Thromboelastography

Venoms were investigated for their ability to affect clot strength ability of plasma and fibrinogen using a Thromboelastography® 5000 using protocols previously described by us (Debono et al., 2018) and (Coimbra et al., 2018; Oulion et al., 2018). Details are as follows.

Using human fibrinogen (4 mg/ml) and human plasma, venoms were investigated using a Thrombelastogram® 5000 Haemostasis analyser (Haemonetics®, Haemonetics Australia Pty Ltd., North Rdye, Sydney 2113, Australia) for their ability in clot strength. Human fibrinogen (4 mg/ml, Lot#F3879, Sigma Aldrich, St. Louis, Missouri, United States) was reconstituted in enzyme buffer (150 mM NaCl and 50 mM Tri-HCl (pH 7.3)). Natural pins and cups (Lot# HMO3163, Haemonetics Australia Pty Ltd., North Rdye, Sydney 2113, Australia) were used with the following solution; 7 μl venom working stock (1 mg/ml in 50% glycerol), 7 μl H_2O in 50% glycerol as a negative control, or 7 μl thrombin as a positive control (stable thrombin from Stago Liquid Fib kit, unknown concentration from supplier (Stago Cat#115081 Liquid Fib)), 72 μl $CaCl_2$ (25 mM stock solution Stago Cat# 00367 STA), 72 μl phospholipid (solubilized in Owren Koller Buffer adapted from STA C·K Prest standard kit, Stago Cat# 00597), and 20 μl Owren Koller Buffer (Stago Cat# 00360) was combined with 189 μl fibrinogen or human plasma and run immediately for 30 mins to allow for ample time for clotting formation. An additional positive control of 7 μl Factor Xa (unknown concentration from supplier, Liquid Anti-Xa FXa Cat#253047, Stago) was also incorporated for plasma only. When no clot was formed from the effects of anticoagulant venoms, an additional 7 μl thrombin was added to the pin and cup to generate a clot and to determine the effects of fibrinogen degradation.

2.3.3. Fibrinogen SDS PAGE electrophoresis and gel image analysis

Venoms from *Azemiops feae, Calloselasma rhodostoma*, *Deinagkistrodon acutus*, *Hypnale hypnale*, *Tropidolaemus subannulatus* and *Tropidolaemus wagleri* were investigated for ability to cleave fibrinogen using protocols previously described by us (Debono et al., 2018; Dobson et al., 2018). Details are as follows.

Human fibrinogen (Lot#F3879, Sigma Aldrich, St. Louis, Missouri, United States) was reconstituted to a concentration of 1 mg/ml in

isotonic saline solution, flash frozen in liquid nitrogen and stored at −80 °C until use. Freeze-dried venom was reconstituted in deionized H_2O and concentrations were measured using a Thermo Fisher Scientific™ NanoDrop 2000 (Waltham, MA, USA). Assay concentrations were a 1:10 ratio of venom:fibrinogen. Human fibrinogen (Lot#F3879, Sigma Aldrich, St. Louis, Missouri, United States) stock of 1 mg/ml was dispensed into ten 120 µl aliquots. Fibrinogen from each aliquot (10 µl) was added to 10 µl buffer dye (5 µl of 4× Laemmli sample buffer (Bio-Rad, Hercules, CA, USA), 5 µl deionized H_2O, 100 mM DTT (Sigma-Aldrich, St. Louis, MO, USA)) as an untreated control lane. An additional fibrinogen aliquot (10 µl) was firstly incubated for 60 mins at 37 °C before immediately adding 10 µl buffer dye. Venom stock (1 µl at 1 mg/ml) was added to the remaining 100 µl fibrinogen aliquot and incubated over 60 mins at 37 °C, taking out 10 µl at varying time points (1, 5, 10, 15, 20, 30, 45 and 60 mins). This 10 µl was immediately added to an additional 10 µl buffer dye. Once all 8-time points including the two controls were added to the buffer dye these were incubated at 100 °C for 4 min then immediately loaded into the precast 1D SDS-PAGE gel. The following set up within the gel was as follows: Lane 1: untreated, unincubated fibrinogen, Lane 2: 1-minute 37 °C incubation, Lane 3: 5 min 37 °C incubation, Lane 4: 10 min 37 °C incubation, Lane 5: 15 min 37 °C incubation, Lane 6: 20 min 37 °C incubation, Lane 7: 30 min 37 °C incubation, Lane 8: 45 min 37 °C incubation, Lane 9: 60 min 37 °C incubation, Lane 10: untreated fibrinogen that has been incubated for 60 min at 37 °C. Gels were prepared in triplicate under the described conditions per venom and were run in 1× gel running buffer (as described by (Debono et al., 2017a; Koludarov et al., 2017) at room temperature at 120 V (Mini Protean3 power-pack from Bio-Rad, Hercules, CA, USA) until the dye front neared the bottom of the gel. Gels were stained with colloidal coomassie brilliant blue G250 (34% methanol (VWR Chemicals, Tingalpa, QLD, Australia), 3% orthophosphoric acid (Merck, Darmstadt, Germany), 170 g/L ammonium sulfate (Bio-Rad, Hercules, CA, USA), 1 g/L Coomassie blue G250 (Bio-Rad, Hercules, CA, USA), and destained in deionized H_2O.

2.4. Fibrinogen gel analysis (ImageJ and PRISM)

Using the publicly available software ImageJ (V1.51r, Java 1.6.0_24, National Institutes of Health, Bethesda, Maryland, USA) (Schneider et al., 2012), gels that had been scanned using a standard printer/scanner were loaded onto the software. Gel images were opened in ImageJ and changed to 32 bit to emphasise darken bands of fibrinogen chains. The 'box function' was then used to draw around the control bands selecting all three chains. This was repeated for all 10 treatment lanes. Lanes were then 'plotted' using the 'plot lanes' function which creates a gel band intensity graph. Using the 'line function', lines were drawn between troughs of each band separating the individual peaks and troughs representing the alpha, beta and gamma chains. The intensity represents the amount of protein within that particular band and as the chain degrades the intensity decreases. Using the 'wand function' each peak within the graph was selected automatically producing a quantity for the area under the curve. These values were entered into Windows Excel 2016, average taken and graphed using GraphPad PRISM 7.0 (GraphPad Prism Inc., La Jolla, CA, USA). This process was repeated for all three triplicates for each venom.

2.4.1. Factor X activation and prothrombin activation

To determine the relative rate of Factor X activation or prothrombin activation by venom samples, a working stock solution (at 1 mg/ml in 50% deionized H_2O + 50% glycerol) was manually diluted with OK buffer (STA Owren Koller Buffer) (50 µl at 20 µg/ml) to a cuvette. A total of 50 µl of $CaCl_2$ (25 mM), 50 µl phospholipid (cephalin prepared from rabbit cerebral tissue from STA C·K Prest standard kit, solubilized in OK buffer) and 25 µl of OK buffer was added to cuvette and incubated for 120 s at 37 °C before adding 75 µl of a solution containing the colorimetric substrate (Liquid Anti-Xa substrate, Stago LOT 253047) and either 0.01 µg/µl FX (Human Factor X, Lot #HH0315, HTI) or 0.1 µg/µl prothrombin (Human Prothrombin, Lot # GG1026, HTI) (total volume 250 µl/cuvette). A change in the optical density (OD) was measured each second for 300 s using a STA-R Max® automated analyser (Stago, Asnières sur Seine, France). All tests were performed in triplicate. The rate of FX activation or prothrombin activation, by the samples, was calculated in comparison to the variation in the optical density – corresponding to the cleavage of the substrate by FXa or thrombin, after the activation of the zymogen by the samples, in relation to direct cleavage of substrate by the samples in the absence of the zymogen. Human FXa (Liquid Anti-Xa FXa LOT 253047) or thrombin (Liquid Fib, Stago, LOT 253337) was used as positive control to ensure quality of the substrate. The samples analyzed, in same conditions, without the presence of the zymogen were used as a negative control to establish and venom-induced baseline substrate cleavage in the absence of the zymogen. A solution containing deionized H_2O/glycerol at a 1:1 ratio was used as a second negative control.

2.4.2. Fibrinolysis

The ability of venoms from *Azemiops feae, Calloselasma rhodostoma*, *Deinagkistrodon acutus*, *Tropidolaemus subannulatus* and *Tropidolaemus wagleri* to activity lyse clots was investigated in the presence or absence of tPA following methods described previously by us (Debono et al., 2018). Details are as follows:

To investigate the fibrinolysis ability of the above venoms, varying concentrations of venom (100 ng/µl, 500 ng/µl and 1 µg/µl) were tested under varying conditions with the addition of tissue plasminogen activator (tPA, Sekisui Diagnostics, Lexington, MA, USA). Aliquots (100 µl) of normal pooled human plasma (Leiden University Medical Center (Leiden, NL)) stored at −80 °C were defrosted in a water bath at 37 °C. A 96-well plate was prepared under the following conditions: 6 pM tissue factor (TF) (Innovin, Siemens, USA) was added to 10 µM phospholipid vesicles (PCPS, 75% phosphatidylcholine and 25% phosphatidylserine, Avanti Polar Lipids, Alabama, USA) in HEPES buffer (25 mM HEPES, 137 mM NaCl, 3.5 mM KCl, 0.1% BSA (Bovine Serum Albumin A7030, Sigma Aldrich, St Louis, MD, USA)) and gently incubated at 37 °C for 1 h in a water bath. 17 mM CaCl and 37.5 U/ml tPA (diluted in dilution buffer (20 mM HEPES, 150 mM NaCl, 0.1% PEG-8000 (Polyethylene glycol 8000,1,546,605 USP, Sigma Aldrich, St Louis, MD, USA), pH 7.5)) was then added to the solution. A volume of 30 µl of this solution was added to each experimental well, along with 10 µl of venom at varying concentrations and an additional 10 µl of HEPES buffer, prepared on ice (total well volume of 100 µl). Normal pooled plasma (50 µl) was immediately added to each well (heated to 37 °C). Absorbance measuring commenced immediately and was measured every 30 s over 3 h at 405 nm on a Spectra Max M2^e (Molecular Devices, Sunnyvale, CA, USA) plate reader, heated to 37 °C. Measurements were captured on Softmax Pro software (V 5.2, Molecular Devices, Sunnyvale, CA, USA) and data points analyzed using GraphPad PRISM 7.0 (GraphPad Prism Inc., La Jolla, CA, USA). All experimental conditions were repeated in triplicates and averaged.

3. Results

3.1. Enzymatic assays

Significant variation was evident upon artificial substrates which are in general cleaved by metalloproteases (ES001, ES003, ES005, ES010), serine proteases (ES002, ES011), or phospholipase A_2 (Fig. 1). For all six venoms, none of the substrates displayed a strong taxonomical signal or a pattern regarding ecological niche occupied (arboreal versus terrestrial). None of the venoms cleaved ES005, and therefore this data is not shown.

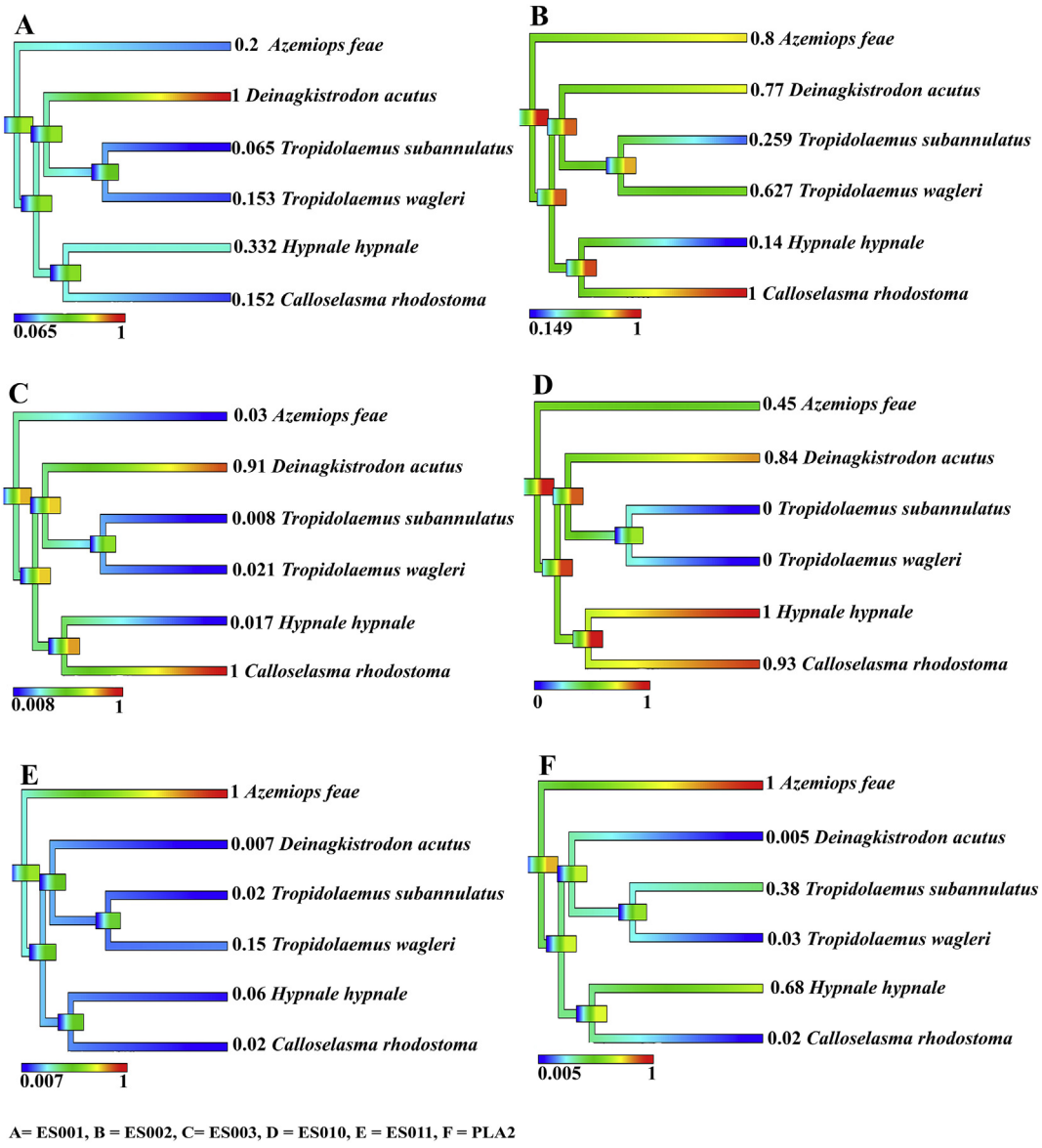

Fig. 1. Ancestral state reconstruction of enzymatic substrate activity of the Basal clade species based on their ability to cleave the following substrates; A: fluorogenic peptide substrate (Mca-PLGL-Dpa-AR-NH2 Fluorogenic Matrix Metalloprotease Substrate, Cat#ES001), B: fluorogenic peptide substrate (Mca-RPKPVE-Nval-WRK (Dnp)-NH2 Fluorogenic MMP Substrate, Cat#ES002) which detects additional metalloprotease activity and Factor X, C: fluorogenic peptide substrate (Mca-PLAQAV-Dpa-RSSSR-NH2 Fluorogenic Peptide Substrate, Cat#ES003) which detects additional metalloprotease activity, D: fluorogenic peptide substrate (Mca-KPLGL-Dpa-AR-NH2 Fluorogenic Peptide Substrate, Cat#ES010) which detects additional metalloprotease activity, E: fluorogenic peptide substrate (Boc-VPR-AMC Fluorogenic Peptide Substrate, Cat#ES011) which detects serine protease activity, F: Phospholipase A_2 substrate activity, EnzChek® (Cat# E10217). Warmer colours represent more potent substrate cleavage. Bars indicate 95% confidence intervals for the estimate at each node. Phylogeny follows (Alencar et al., 2016).

3.2. Coagulation analysis: human plasma and fibrinogen

At the initial 20 μg/ml venom concentration, only *C. rhodostoma* (20.5 ± 2.6 s), *D. acutus* (41.9 ± 0.5) and *H. hypnale* displayed the ability to clot plasma quicker than the negative control (spontaneous clotting of recalcified plasma) time of 300 ± 50 s (Fig. 2). All other species were equal or above the negative control. 8-point dilution series were undertaken with the two most potent venoms (*C. rhodostoma* and *D. acutus*) under three experimental conditions: with both cofactors (calcium and phospholipid), with just calcium, and with just phospholipid. While the phospholipid cofactor was not a significant variable for either venom, for calcium there was an area under the curve shift of 79.3 ± 4% for *D. acutus* and a shift of 49.1 ± 1% for *C. rhodostoma* (if there was no shift in the area under the curve, the value would have been zero) (Fig. 2). 8-point dilution series were also undertaken for *C. rhodostoma* and *D. acutus* with fibrinogen under three experimental conditions: with both cofactors (calcium and phospholipid), with just calcium, and with just phospholipid (Fig. 3). While phospholipid was again not a significant variable for either venom, there was a strong dependency evident for calcium, with the area of the curve shifting 123.1 ± 15.2% for *C. rhodostoma* and 345.1 ± 5.4% *D. acutus* (if there was no shift in the area under the curve, the value would have been zero) (Fig. 3).

3.3. Thromboelastography: plasma and fibrinogen

Thromboelastography studies on plasma (Fig. 4) revealed that while *C. rhodostoma* and *D. acutus* both rapidly clotted plasma, consistent with the coagulation analyser results above, only *C. rhodostoma* formed strong, stable clots and therefore was truly procoagulant. Similarly, *H.*

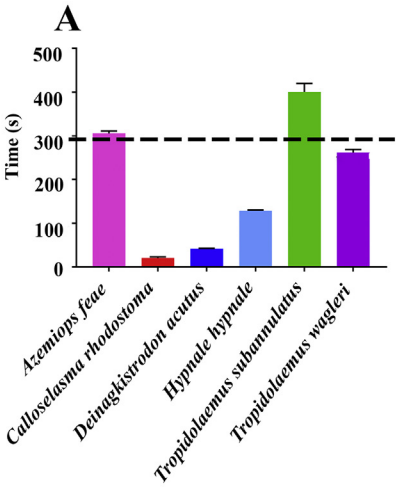

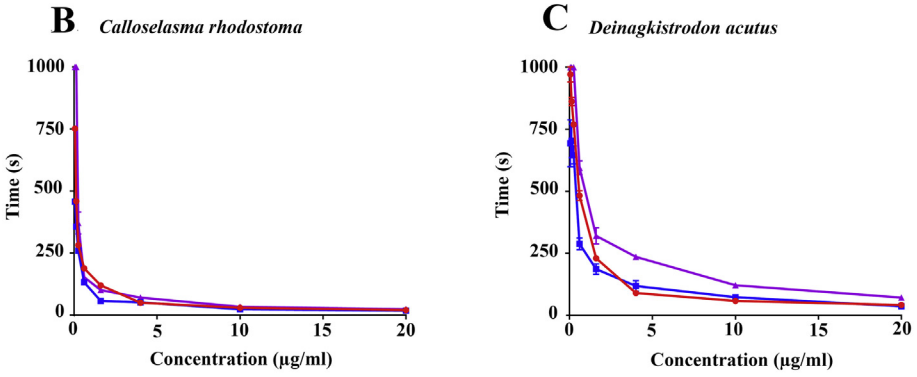

Fig. 2. A) Effect of 20 µg/ml venom concentration upon plasma clotting relative to the negative control (spontaneous clotting of recalcified plasma, shown with dashed line) time of 300 ± 50 s. Also shown are 8-point dose-response curves with both calcium and phospholipid (red line), with just calcium (blue line), and with just phospholipid (purple line) for B) *C. rhodostoma* and C) *D. acutus*. Data points are $N = 3$ with standard deviations. Note that for the line graphs in (B) and (C) the error bars are in some cases smaller than the line icons. (For interpretation of the references to colour in this figure legend, the reader is referred to the web version of this article.)

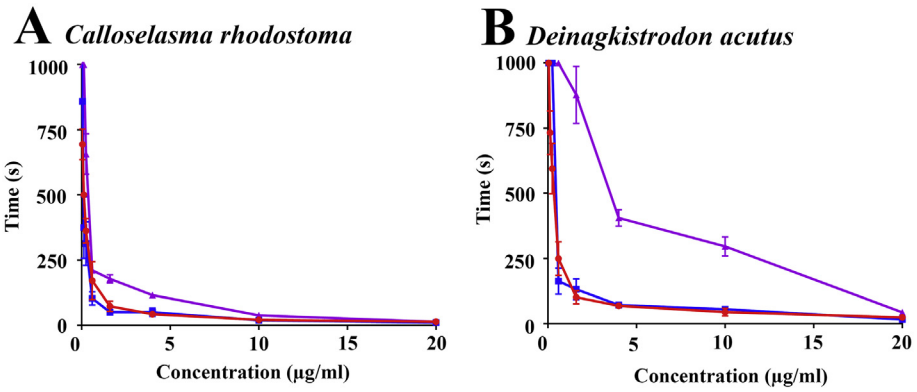

Fig. 3. 8-point dose-response curves of fibrinogen clotting activity with both calcium and phospholipid (red line), with just calcium (blue line), and with just phospholipid (purple line) for A) *C. rhodostoma* and B) *D. acutus*. Data points are N = 3 with standard deviations. (For interpretation of the references to colour in this figure legend, the reader is referred to the web version of this article.)

hypnale also formed strong stable clots despite being much slower to clot plasma in the above analyses. In contrast, *D. acutus* rapidly formed weak, unstable clots and therefore was pseudo-procoagulant. None of the other venoms differed significantly from the spontaneous clotting negative control. Thromboelastography studies on fibrinogen (Fig. 5) revealed *C. rhodostoma* to also have the ability directly clot fibrinogen in a pseudo-procoagulant manner, in contrast to its ability to act in a true procoagulant manner and generate endogenous thrombin (with thrombin in further stabilising the clots by activating FXIII). Consistent with the plasma results, *D. acutus* displayed the ability to clot fibrinogen in a pseudo-procoagulant manner while *H. hypnale* showed only a weak ability. *T. wagleri* also showed a weak ability to clot fibrinogen in a pseudo-procoagulant manner while its sister species *T. subannulatus* displayed a weak ability to cleave fibrinogen in a non-clotting, destructive manner. *A. feae* neither clotted nor destroyed fibrinogen.

3.4. FX activation and prothrombin activation

As *C. rhodostoma, H. hypnale* and *D.acutus* displayed clotting ability, they were investigated for their ability activate FX and prothrombin, to establish if they generated endogenous thrombin and therefore were true procoagulant venoms. *C. rhodostoma* activated FX yet the only minimal activity was recorded for *H. hypnale* from the sister genus *Hypnale,* and no activity was recorded for *D. acutus* (Fig. 6). There was no activity recorded for prothrombin activation by any species (*data not shown*).

3.5. Fibrinolysis ± tPA

The ability for species' venoms within the basal clade to actively lyse tissue factor-induced plasma clots was tested at varying venom concentrations. None of the species tested returned a positive result of

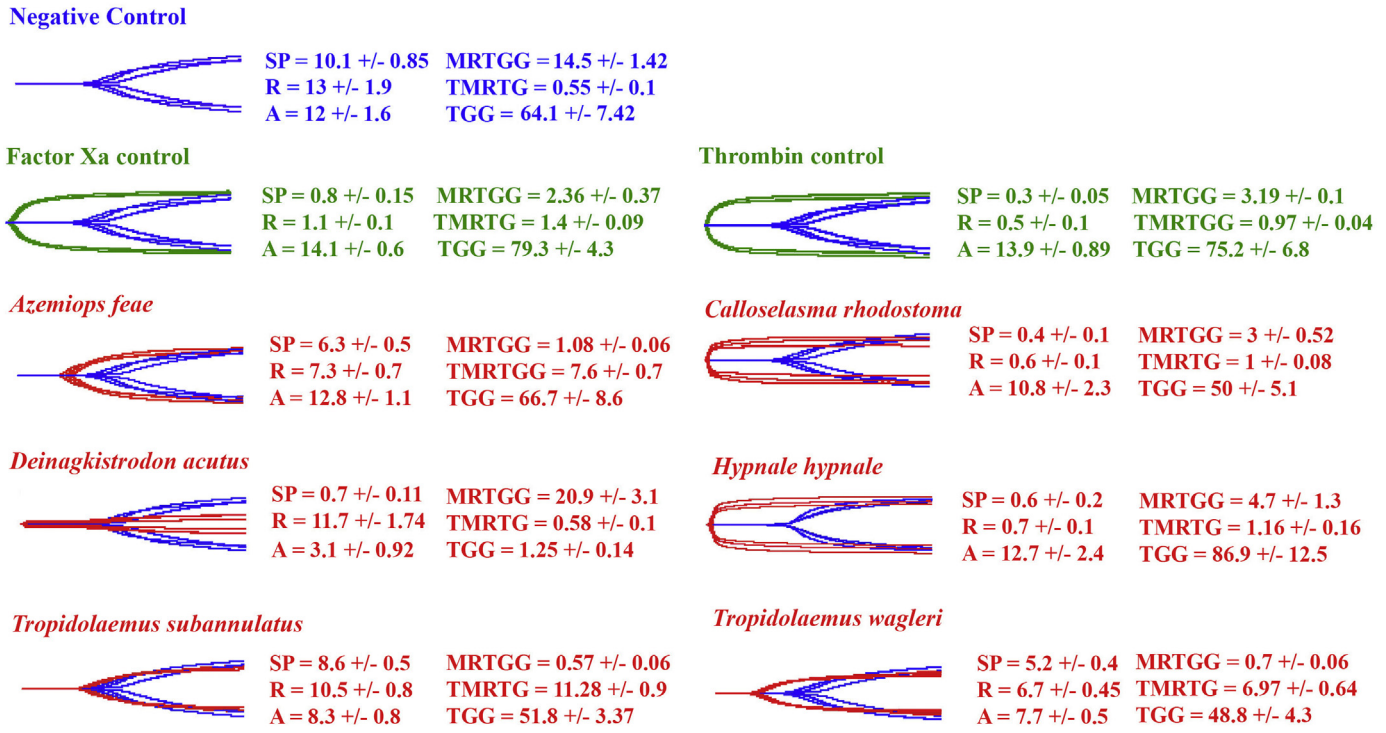

Fig. 4. Overlaid thromboelastography traces showing effects of venoms ability to clot plasma relative to spontaneous clot control where species cleave plasma in a clotting manner to form weak clots. Blue traces = spontaneous clot controls, green traces = thrombin induced clot or Factor Xa induced clot, red traces = samples. SP = split point, time taken until clot begins to form (mins). R = time to initial clot formation where formation is 2 mm + (mins). A = amplitude of detectable clot (mm).. MRTGG = maximum rate of thrombus generation (dsc, dynes/cm^2/s). TMRTG = time to maximum rate of thrombus generation (min). TGG = total thrombus generation (dynes/cm^2).. Overlaid traces are N = 3 for each set of control or experimental conditions. Values are N = 3 means and standard deviation. (For interpretation of the references to colour in this figure legend, the reader is referred to the web version of this article.)

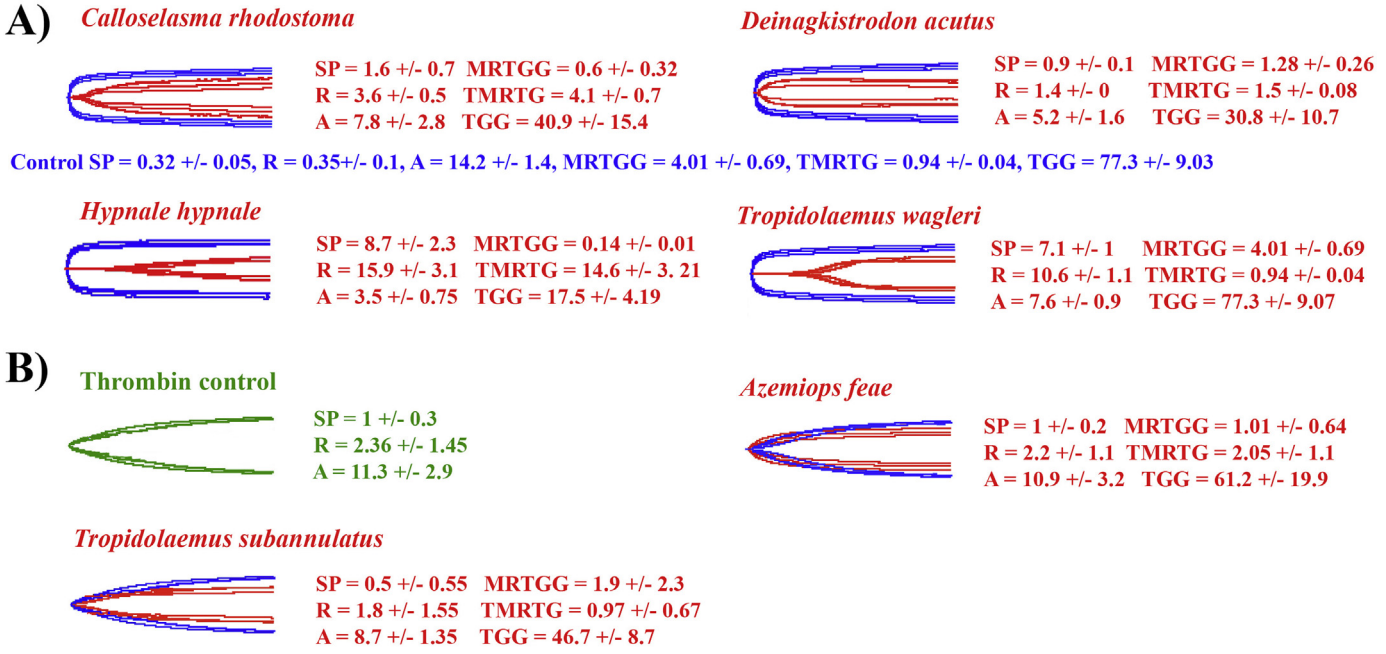

Fig. 5. Overlaid thromboelastography traces showing tests for A) ability to clot fibrinogen relative to thrombin control; or B) test for the ability to degrade fibrinogen for species which did not clot in (A) whereby thrombin was added at the end of the 30 min runs to test for intact fibrinogen. Green traces = thrombin controls, red traces = samples. SP = split point, time taken until clot begins to form (mins). R = time to initial clot formation where formation is 2 mm + (mins). A = amplitude of detectable clot (mm).. MRTGG = maximum rate of thrombus generation (dynes/cm^2/s). TMRTG = time to maximum rate of thrombus generation (min). TGG = total thrombus generation (dynes/cm^2).. Overlaid traces are N = 3 for each set of control or experimental conditions. Values are N = 3 means and standard deviation. (For interpretation of the references to colour in this figure legend, the reader is referred to the web version of this article.)

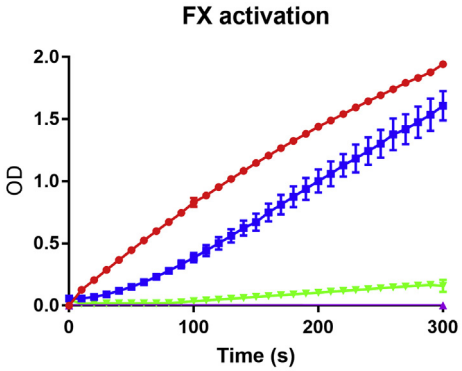

Fig. 6. Factor X activation via colourimetric analysis over time performed on a Stage STA R Max. Y axis = OD, optical density, X axis = time (secs). Red line = control FXa, blue line = *Calloselasma rhodostoma*, green line = *Hypnale hypnale*, purple line = *Deinagkistrodon acutus*. Data points are $n = 3$, means and SD. (For interpretation of the references to colour in this figure legend, the reader is referred to the web version of this article.)

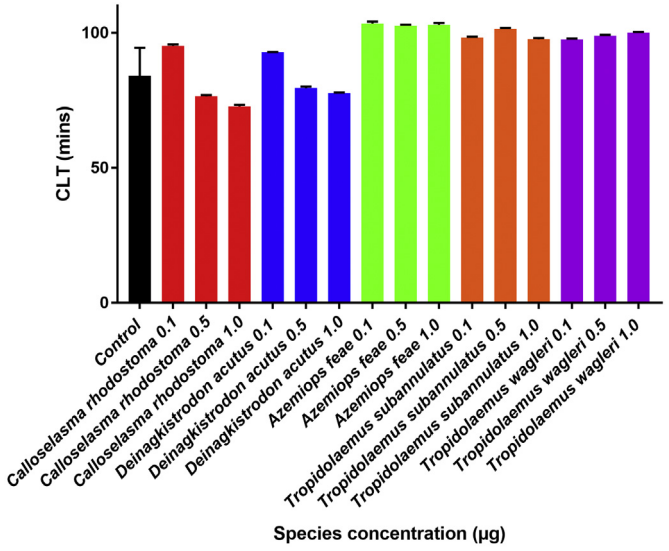

Fig. 7. Clot Lysis Time (CLT) for each species within the basal clade in the presence of tPA at 0.1 µg, 0.5 µg and 1 µg venom concentrations. Control is indicated in black. Columns are averages of triplicates and error bars given for each. Bars which are lower than the control lysed the plasma clot quicker than under normal tPA conditions.

lysing a clot. However compared to a normal clot lysis time (CLT), this was decreased in the presence of *C. rhodostoma* and *D. acutus* venoms and tPA (Fig. 7).

3.6. Fibrinogen gels

Time-dependent cleavage of fibrinogen chains was also investigated using electrophoresis. Venom from *Azemiops feae* failed to cleave any of the fibrinogen, while *Tropidolaemus wagleri* and *Hypnale hypnale* cleaved all 3 chains within 30 min (Figs. 8 and 9). Venom from *Calloselasma rhodostoma*, *Tropidolaemus subannulatus* and *Deinagkistrodon acutus* all cleaved the alpha chain rapidly, while slowly cleaving the beta chain but with no effect on the gamma chain (Figs. 8 and 9).

4. Discussion

The venoms within the clade studied here, formed by the genera *Azemiops, Calloselasma, Hypnale, Deinagkistrodon,* and *Tropidolaemus*, were as functionally diverse as the snakes are themselves in morphology and ecological niche occupied, with the snakes ranging from semi-fossorial species, to ambush feeding, heavily camouflaged terrestrial, to arboreal species. There were no phylogenetic or ecological patterns in their actions upon enzymatic substrates (Fig. 1) or in the functional tests. The camouflaged, sit and wait ambush specialists (*C. rhodostoma, H. hypnale* and *D. acutus*) were similar in that they clotted plasma and fibrinogen (Figs. 2–5), but the underlying mechanics were starkly different.

Consistent with previous reports of this venom (Ainsworth et al., 2018; Nielsen and Bazzell, 2017; Yamada et al., 1997) *C. rhodostoma* was a true procoagulant venom. In this study it was shown to activate Factor X generating endogenous thrombin, forming a strong, stable fibrin clot which would be further stabilised by the endogenous thrombin activating FXIII. In contrast, *H. hypnale* venom produced a strong stable clot upon plasma but did not activate Factor X or Prothrombin and formed a very weak, unstable clot when tested on fibrinogen (Figs. 4–6). *D. acutus* venom, however, was shown to be pseudo-procoagulant in that it acted directly upon fibrinogen to produce transient, weak fibrin clots (Figs. 4 and 5).

C. rhodostoma retained the ability to directly clot fibrinogen in a pseudo-procoagulant manner, however this action was significantly slower than the true-procoagulant action of Factor X activation, resulting in the generation of endogenous thrombin which would create strong, stable clots further reinforced by thrombin's activation of FXIII (Fig. 5). Therefore, prey subjugation would be facilitated through the induction of stroke, as has been seen convergently for other venoms, not only other vipers such *Echis* (Rogalski et al., 2017) and *Bothrops* (Sousa et al., 2018) but also diverse snakes from other families such as *Dispholidus* and *Thelatornis* with the Colubridae (Debono et al., 2017a), *Hoplocephalus, Notechis, Paroplocephalus* and *Tropidechis* within the Elapidae (Lister et al., 2017), and *Atractaspis* within the Lamprophiidae (Oulion et al., 2018). However, in human bite victims the larger blood volume would dilute the venom and lessen the likelihood of large blood clots forming. Instead there would be a depletion of fibrinogen and clotting factors, as a consequence of endogenous thrombin generation which would result in a venom induced consumptive coagulopathy (VICC), creating a net anticoagulant state (Isbister, 2010). Therefore, while prey items which rapidly succumb due to venom-inducted stroke, the longer survival of envenomed humans would allow sufficient time for potentiation of the net anticoagulation effects due to the secondary action upon the remaining fibrinogen - the pseudo-procoagulant cleavage to form weak, transient clots with remaining fibrinogen (Ho et al., 1986; Tang et al., 2016; Warrell et al., 1986).

In contrast, the transient, weak fibrin clots shown in this study for *D. acutus* venom, consistent with previous reports (Nielsen and Frank, 2018) would have a short half-life due to their inherent instability. Thus the effects upon both prey and humans envenomated by *D. acutus* venoms would therefore be similar: a rapid decrease in fibrinogen levels leading to an anticoagulant state (Cheng et al., 2017; Ouyang and Teng, 1976, 1978), with death resulting from haemorrhagic shock, like has been shown for the *Protobothrops* genus (Debono et al., 2018). Both *D. acutus* and *H. hypnale* venoms displayed similar biochemistry for their pseudo-procoagulant action, which required calcium for full action (Nielsen, 2016a; Nielsen and Bazzell, 2017). The activity that *H. hypanle* displays upon plasma still remains a mystery, as the venom does not activate Factor X or Prothrombin (Fig. 6). Additional investigation into the mechanisms behind this activity would be the focus of future research, such as activation of other clotting factors (ie IX or XI).

Of the other species within this study, in the thromboelastography studies, only *T. wagleri* displayed evidence of action upon fibrinogen, showing only a moderate level of pseudo-procoagulant activity, yet its sister species *T. subannulatus* did not display such activity. *A. feae* also did not display any coagulotoxic action. The low to non-existent coagulotoxic activity is consistent with *Azemiops* and *Tropidolaemus* both known to have contain novel neurotoxic peptides rather than the larger enzymes typical of viperid venoms (Schmidt and Weinstein, 1995;

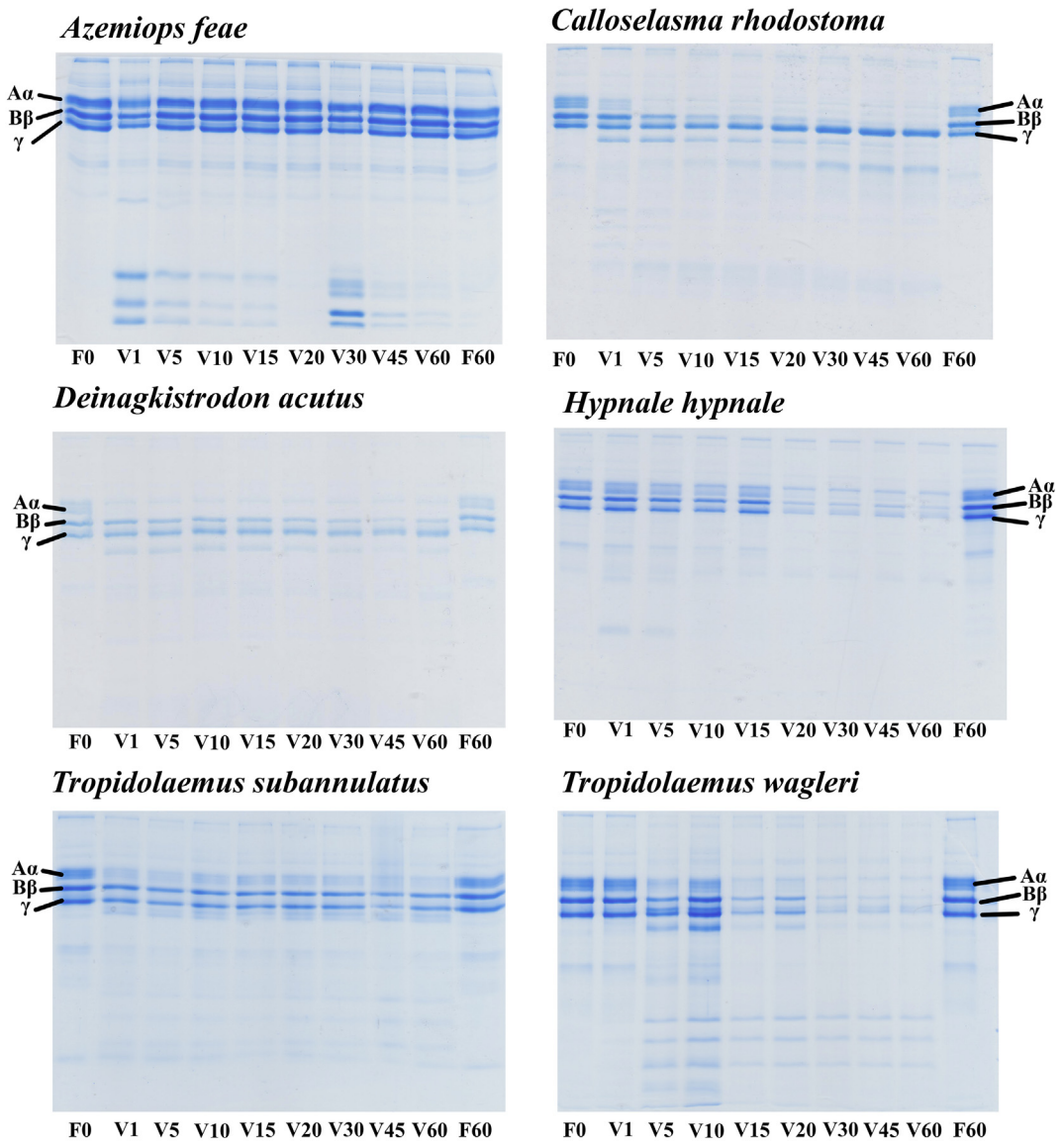

Fig. 8. 1D SDS PAGE time dependent fibrinogen chain degradation (α, β or γ) by venom at 0.1 μg/μl concentration at 37 °C over 60 mins. F = fibrinogen at 0 mins or 60 mins incubation controls, V = venom at 1, 5… 60 min incubation.

Shelukhina et al., 2018; Tan et al., 2017). In both cases, it has been shown that the neurotoxic peptides emerged in the venoms from de novo evolution of novel bioactive peptides in the propeptide-region of the venom forms of C-type natriuretic peptides (Brust et al., 2013; Debono et al., 2017b). However, as these genera are not sister to each other and occupy very different ecological niches (semi-fossorial for *Azemiopis* and arboreal for *Tropidolaemus*) the selection pressure for the molecular evolution of the peptides was differential.

The functional variation extended to the patterns of fibrinogen chain cleavage as revealed in the SDS PAGE gels (Figs. 8 and 9). *C. rhodostoma* and *D. acutus* were similar in rapidly cleaving the A-alpha and B-beta chains but not the gamma, which is consistent with both venoms having the ability for pseudo-procoagulant direct action upon fibrinogen (Fig. 5). *T. wagleri* was the only other venom to display significant action in the fibrinogen thromboelastography studies, having a moderate pseudo-procoagulant activity (Fig. 5), and this venom cleaved all three fibrinogen chains (Figs. 8 and 9). The sister species *T. subannulatus* displayed a similar, but weaker, activity on the fibrinogen gels (Figs. 8 and 9) despite not having a significant functional activity in the venom concentration tested in the thromboelastography studies (Fig. 5). Consistent with the functional studies (Fig. 5), *A. feae* did not have any activity on the fibrinogen gels (Figs. 8 and 9).

Just as the neurotoxicity exhibited by some species in this clade of snakes are unique, so too is the thrombin generating activity of *C. rhodostoma.* In contrast, *D. acutus* was more like the typical Asian pit-viper, which are broadly known for their haemorrhagic-shock inducing venoms (Cheng et al., 2017; Debono et al., 2018; Hutton et al., 1990; Joseph et al., 2007; Maduwage et al., 2013a; Rojnuckarin et al., 1998; Warrell et al., 1986; Withana et al., 2014). Haemorrhagic effects are a result of anticoagulation mechanisms, or a net anticoagulant outcome. As previously mentioned, haemorrhagic effects were demonstrated within this group as irregular degradation of fibrinogen chains, which creates weak clots such as was evident for the *D. acutus* venom in the thromboelastography studies (Figs. 4 and 5). Such degradation of fibrinogen has previously been shown with the isolation and purification of a 'thrombin-like enzyme' (TLE) 'Ancrod' from *C. rhodostoma*, a serine protease which is able to cleave α from Aα chain (Markland, 1998; Nolan et al., 1976; Vaiyapuri et al., 2015).

An in-depth investigation into these mechanisms controlling coagulation has somewhat been neglected from the literature, and a thorough analysis into the actions upon the blood system is required. The addition of co-factor analysis and dependency is extremely

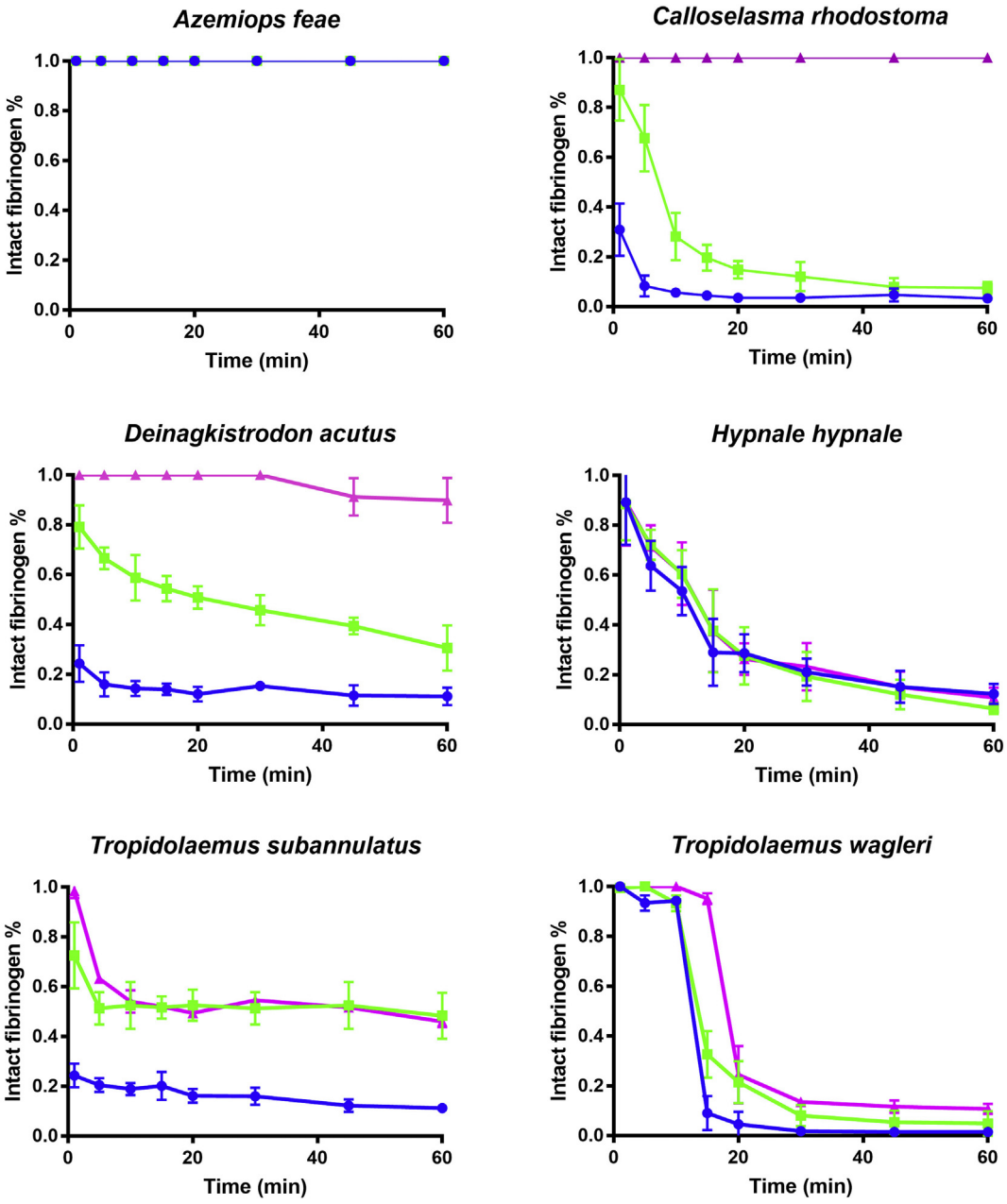

Fig. 9. Relative cleavage of alpha (blue), beta (green) or gamma (pink) chains of fibrinogen. X-axis is time (min), y-axis is percentage of intact chain remaining. Error bars indicate standard deviation and N = 3 means. (For interpretation of the references to colour in this figure legend, the reader is referred to the web version of this article.)

important when investigating these lineages, and the true representation of either a procoagulant or anticoagulant action can be demonstrated. Applying this knowledge and gaining a more complete understanding of venom diversification and evolution is important for predictions of potential clinical effects and evidence-based management strategies, in addition to biodiscovery research.

Acknowledgements

BGF was funded by Australian Research Council Discovery Project DP190100304. HFK was supported by the Science and Technology Development Fund of Macau SAR (FDCT) [019/2017/A1].

References

Ainsworth, S., Slagboom, J., Alomran, N., Pla, D., Alhamdi, Y., King, S.I., Bolton, F.M., Gutiérrez, J.M., Vonk, F.J., Toh, C.-H., Calvete, J.J., Kool, J., Robert, H.A., Casewell, N.R., 2018. The paraspecific neutralisation of snake venom induced coagulopathy by antivenoms. Commun. Biol. 1, 34.

Alencar, L.R., Quental, T.B., Grazziotin, F.G., Alfaro, M.L., Martins, M., Venzon, M., Zaher, H., 2016. Diversification in vipers: phylogenetic relationships, time of divergence and shifts in speciation rates. Mol. Phylogenet. Evol. 105, 50–62.

Alencar, L.R., Martins, M., Greene, H.W., 2018. Evolutionary History of Vipers. eLS. pp. 1–10.

Ali, S.A., Baumann, K., Jackson, T.N., Wood, K., Mason, S., Undheim, E.A., Nouwens, A., Koludarov, I., Hendrikx, I., Jones, A., Fry, B., 2013. Proteomic comparison of *Hypnale hypnale* (hump-nosed pit-viper) and *Calloselasma rhodostoma* (Malayan pit-viper) venoms. J. Proteome 91, 338–343.

Alirol, E., Sharma, S.K., Bawaskar, H.S., Kuch, U., Chappuis, F., 2010. Snake bite in South Asia: a review. PLoS Negl. Trop. Dis. 4, e603.

Ariaratnam, C., Thuraisingam, V., Kularatne, S., Sheriff, M., Theakston, R.D.G., De Silva, A., Warrell, D., 2008. Frequent and potentially fatal envenoming by hump-nosed pit vipers (Hypnale hypnale and H. Nepa) in Sri Lanka: lack of effective antivenom.

Trans. R. Soc. Trop. Med. Hyg. 102, 1120–1126.
Brust, A., Sunagar, K., Undheim, E.A., Vetter, I., Yang, D.C., Casewell, N.R., Jackson, T.N., Koludarov, I., Alewood, P.F., Hodgson, W.C., 2013. Differential evolution and neofunctionalization of snake venom metalloprotease domains. Mol. Cell. Proteomics 12, 651–663.
Cheng, C.-L., Mao, Y.-C., Liu, P.-Y., Chiang, L.-C., Liao, S.-C., Yang, C.-C., 2017. *Deinagkistrodon acutus* envenomation: a report of three cases. J. Venom. Anim. Toxins Incl. Trop. Dis. 23, 20.
Coimbra, F.C., Dobson, J., Zdenek, C.N., Op den Brouw, B., Hamilton, B., Debono, J., Masci, P., Frank, N., Ge, L., Kwok, H.F., Fry, B.G., 2018. Does size matter? Venom proteomic and functional comparison between night adder species (Viperidae: *Causus*) with short and long venom glands. Comp. Biochem. Physiol. Part C 211, 7–14.
Daltry, J.C., Ponnudurai, G., Shin, C.K., Tan, N.-h., Thorpe, R.S., Wolfgang, W., 1996. Electrophoretic profiles and biological activities: intraspecific variation in the venom of the Malayan pit viper (*Calloselasma rhodostoma*). Toxicon 34, 67–79.
Dambisya, Y.M., Lee, T.-L., Gopalakrishnakone, P., 1994. Action of *Calloselasma rhodostoma* (Malayan pit viper) venom on human blood coagulation and fibrinolysis using computerized thromboelastography (CTEG). Toxicon 32, 1619–1626.
de Silva, A., Wijekoon, A., Jayasena, L., Abeysekera, C., Bao, C.-X., Button, R., Warrell, D., 1994. Haemostatic dysfunction and acute renal failure following envenoming by Merrem's hump-nosed viper (*Hypnale hypnale*) in Sri Lanka: first authenticated case. Trans. R. Soc. Trop. Med. Hyg. 88, 209–212.
Debono, J., Dobson, J., Casewell, N.R., Romilio, A., Li, B., Kurniawan, N., Mardon, K., Weisbecker, V., Nouwens, A., Kwok, H.F., Fry, B.G., 2017a. Coagulating colubrids: evolutionary, pathophysiological and biodiscovery implications of venom variations between boomslang (*Dispholidus typus*) and twig snake (*Thelotornis mossambicanus*). Toxins 9, 171.
Debono, J., Xie, B., Violette, A., Fourmy, R., Jaeger, M., Fry, B.G., 2017b. Viper venom botox: the molecular origin and evolution of the waglerin peptides used in anti-wrinkle skin cream. J. Mol. Evol. 84, 8–11.
Debono, J., Bos, M.H., Nouwens, A., Ge, L., Frank, N., Kwok, H.F., Fry, B., 2018. Habu coagulotoxicity: clinical implications of the functional diversification of *Protobothrops* snake venoms upon blood clotting factors. Toxicol. in Vitro 55, 62–74.
Dharmaratne, L., Gunawardena, U., 1988. Generalised bleeding tendency and acute renal ailure following Merrem's hump-nosed viper bite. J. Ceylon. Coll. Physns. 21, 37–42.
Dobson, J., Yang, D.C., Op den Brouw, B., Cochran, C., Huynh, T., Kurrupu, S., Sánchez, E.E., Massey, D.J., Baumann, K., Jackson, T.N., 2018. Rattling the border wall: pathophysiological implications of functional and proteomic venom variation between Mexican and US subspecies of the desert rattlesnake *Crotalus scutulatus*. Comp. Biochem. Physiol. Part C 205, 62–69.
Esnouf, M., Tunnah, G., 1967. The isolation and properties of the thrombin-like activity from *Agkistrodon rhodostoma* venom. Br. J. Haematol. 13, 581–590.
Fry, B.G., 2018. Snakebite: when the human touch becomes a bad touch. Toxins 10, 170.
Fry, B.G., Roelants, K., Champagne, D.E., Scheib, H., Tyndall, J.D., King, G.F., Nevalainen, T.J., Norman, J.A., Lewis, R.J., Norton, R.S., Renjifo, C., Rodríguez de la Vega, R.C., 2009. The toxicogenomic multiverse: convergent recruitment of proteins into animal venoms. Annu. Rev. Genomics Hum. Genet. 10, 483–511.
Gutiérrez, J.M., Theakston, R.D.G., Warrell, D.A., 2006. Confronting the neglected problem of snake bite envenoming: the need for a global partnership. PLoS Med. 3, e150.
Herath, N., Wazil, A., Kularatne, S., Ratnatunga, N., Weerakoon, K., Badurdeen, S., Rajakrishna, P., Nanayakkara, N., Dharmagunawardane, D., 2012. Thrombotic microangiopathy and acute kidney injury in hump-nosed viper (*Hypnale* species) envenoming: a descriptive study in Sri Lanka. Toxicon 60, 61–65.
Ho, M., Warrell, D.A., Looareesuwan, S., Phillips, R.E., Chanthavanich, P., Karbwang, J., Supanaranond, W., Viravan, C., Hutton, R.A., Vejcho, S., 1986. Clinical significance of venom antigen levels in patients envenomed by the Malayan pit viper (*Calloselasma rhodostoma*). Am. J. Trop. Med. Hyg. 35, 579–587.
Huang, T.-F., Chang, M.-C., Peng, H.-C., Teng, C.-M., 1992. A novel α-type fibrinogenase from *Agkistrodon rhodostoma* snake venom. Biochimica et Biophysica Acta (BBA) Protein Structu. Mol. Enzymol. 1160, 262–268.
Hutton, R., Looareesuwan, S., Ho, M., Silamut, K., Chanthavanich, P., Karbwang, J., Supanaranond, W., Vejcho, S., Viravan, C., Phillips, R., 1990. Arboreal green pit vipers (genus *Trimeresurus*) of south-east Asia: bites by *T. albolabris* and *T. macrops* in Thailand and a review of the literature. Trans. R. Soc. Trop. Med. Hyg. 84, 866–874.
Isbister, G.K., 2009. Procoagulant Snake Toxins: Laboratory Studies, Diagnosis, and Understanding Snakebite Coagulopathy, Seminars in Thrombosis and Hemostasis. © Thieme Medical Publishers, pp. 093–103.
Isbister, G.K., 2010. Snakebite doesn't cause disseminated intravascular coagulation: coagulopathy and thrombotic microangiopathy in snake envenoming. Semin. Thromb. Hemost. 36, 444–451.
Joseph, J., Simpson, I., Menon, N., Jose, M., Kulkarni, K., Raghavendra, G., Warrell, D., 2007. First authenticated cases of life-threatening envenoming by the hump-nosed pit viper (*Hypnale hypnale*) in India. Trans. R. Soc. Trop. Med. Hyg. 101, 85–90.
Koludarov, I., Jackson, T.N., Dobson, J., Dashevsky, D., Arbuckle, K., Clemente, C.J., Stockdale, E.J., Cochran, C., Debono, J., Stephens, C., Panagides, N., Li, B., Manchadi, M.-L.R., Violette, A., Fourmy, R., Hendrikx, I., Nouwens, A., Clements, J., Martelli, P., Kwok, H.F., Fry, B.G., 2017. Enter the dragon: the dynamic and multifunctional evolution of Anguimorpha lizard venoms. Toxins 9, 242.
Kong, C., Chung, M.C., 2001. Purification and characterization of a variant of rhodocetin from *Calloselasma rhodostoma* (Malayan pit viper) venom. J. Protein Chem. 20, 383–390.
Leong, P.K., Tan, C.H., Sim, S.M., Fung, S.Y., Sumana, K., Sitprija, V., Tan, N.H., 2014. Cross neutralization of common southeast Asian viperid venoms by a Thai polyvalent snake antivenom (Hemato Polyvalent Snake Antivenom). Acta Trop. 132, 7–14.
Levy, D.E., Del Zoppo, G.J., 2006. Ancrod: a potential treatment for acute, ischemic stroke from snake venom. Toxin Rev. 25, 323–333.
Lister, C., Arbuckle, K., Jackson, T.N., Debono, J., Zdenek, C.N., Dashevsky, D., Dunstan, N., Allen, L., Hay, C., Bush, B., Gillett, A., Fry, B.G., 2017. Catch a tiger snake by its tail: differential toxicity, co-factor dependence and antivenom efficacy in a procoagulant clade of Australian venomous snakes. Comp. Biochem. Physiol. Part C 202, 39–54.
Maduwage, K., Isbister, G.K., Silva, A., Bowatta, S., Mendis, S., Gawarammana, I., 2013a. Epidemiology and clinical effects of hump-nosed pit viper (genus: *Hypnale*) envenoming in Sri Lanka. Toxicon 61, 11–15.
Maduwage, K., Scorgie, F., Silva, A., Shahmy, S., Mohamed, F., Abeysinghe, C., Karunathilake, H., Lincz, L., Gnanathasan, C.A., Isbister, G., 2013b. Hump-nosed pit viper (*Hypnale hypnale*) envenoming causes mild coagulopathy with incomplete clotting factor consumption. Clin. Toxicol. 51, 527–531.
Markland, F.S., 1998. Snake venoms and the hemostatic system. Toxicon 36, 1749–1800.
Mebs, D., Kuch, U., Meier, J., 1994. Studies on venom and venom apparatus of Fea's viper, *Azemiops feae*. Toxicon 32, 1275–1278.
Navdaev, A., Lochnit, G., Eble, J.A., 2011. The rhodocetin αβ subunit targets GPIb and inhibits von Willebrand factor induced platelet activation. Toxicon 57, 1041–1048.
Nielsen, V., 2016a. Iron and carbon monoxide prevent degradation of plasmatic coagulation by thrombin-like activity in rattlesnake venom. Hum. Exp. Toxicol. 35, 1116–1122.
Nielsen, V.G., 2016b. Ancrod revisited: viscoelastic analyses of the effects of *Calloselasma rhodostoma* venom on plasma coagulation and fibrinolysis. J. Thromb. Thrombolysis 42, 288–293.
Nielsen, V.G., Bazzell, C.M., 2017. Carbon monoxide releasing molecule-2 inhibition of snake venom thrombin-like activity: novel biochemical “brake”? J. Thromb. Thrombolysis 43, 203–208.
Nielsen, V.G., Frank, N., 2018. Differential heme-mediated modulation of *Deinagkistrodon*, *Dispholidus*, *Protobothrops* and *Pseudonaja* hemotoxic venom activity in human plasma. Biometals 1–9.
Nolan, C., Hall, L., Barlow, G., 1976. Ancrod, the Coagulating Enzyme from Malayan Pit Viper (*Agkistrodon rhodostoma*) Venom, Methods in Enzymology. Elsevier, pp. 205–213.
Oulion, B., Dobson, J.S., Zdenek, C.N., Arbuckle, K., Lister, C., Coimbra, F.C., Op den Brouw, B., Debono, J., Rogalski, A., Violette, A., Fourmy, R., Frank, N., Fry, B.G., 2018. Factor X activating *Atractaspis* snake venoms and the relative coagulotoxicity neutralising efficacy of African antivenoms. Toxicol. Lett. 288, 119–128.
Ouyang, C., Teng, C.-M., 1976. The effects of the purified thrombin-like and anticoagulant principles of *Agkistrodon acutus* venom on blood coagulation in vivo. Toxicon 14, 49–54.
Ouyang, C., Teng, C.-M., 1978. In vivo effects of the purified thrombin-like and anticoagulant principles of *Agkistrodon acutus* (hundred pace snake) venom. Toxicon 16, 583–593.
Paradis, E., Claude, J., Strimmer, K., 2004. APE: analyses of phylogenetics and evolution in R language. Bioinformatics 20, 289–290.
Premawardena, A., Seneviratne, S., Gunatilake, S., De Silva, H., 1998. Excessive fibrinolysis: the coagulopathy following Merrem's hump-nosed viper (*Hypnale hypnale*) bites. Am. J. Trop. Med. Hyg. 58, 821–823.
Revell, L.J., 2012. Phytools: an R package for phylogenetic comparative biology (and other things). Methods Ecol. Evol. 3, 217–223.
Rogalski, A., Soerensen, C., Op den Brouw, B., Lister, C., Dashevsky, D., Arbuckle, K., Gloria, A., Zdenek, C.N., Casewell, N.R., Gutierrez, J.M., Wuster, W., Ali, S.A., Masci, P., Rowley, P., Frank, N., Fry, B.G., 2017. Differential procoagulant effects of saw-scaled viper (Serpentes: Viperidae: Echis) snake venoms on human plasma and the narrow taxonomic ranges of antivenom efficacies. Toxicol. Lett. 280, 159–170.
Rojnuckarin, P., Mahasandana, S., Intragumthornchai, T., Sutcharitchan, P., Swasdikul, D., 1998. Prognostic factors of green pit viper bites. Am. J. Trop. Med. Hyg. 58, 22–25.
Schmidt, J.J., Weinstein, S.A., 1995. Structure-function studies of waglerin I, a lethal peptide from the venom of Wagler's pit viper, *Trimeresurus wagleri*. Toxicon 33, 1043–1049.
Schneider, C.A., Rasband, W.S., Eliceiri, K.W., 2012. NIH image to ImageJ: 25 years of image analysis. Nat. Methods 9, 671.
Shelukhina, I.V., Zhmak, M.N., Lobanov, A.V., Ivanov, I.A., Garifulina, A.I., Kravchenko, I.N., Rasskazova, E.A., Salmova, M.A., Tukhovskaya, E.A., Rykov, V.A., 2018. Azemiopsin, a selective peptide antagonist of muscle nicotinic acetylcholine receptor: preclinical evaluation as a local muscle relaxant. Toxins 10, 34.
Shin, Y., Morita, T., 1998. Rhodocytin, a functional novel platelet agonist belonging to the heterodimeric C-type lectin family, induces platelet aggregation independently of glycoprotein Ib. Biochem. Biophys. Res. Commun. 245, 741–745.
Sousa, L., Zdenek, C., Dobson, J., Coimbra, F., Gillett, A., Del-Rei, T., Chalkidis, H., Sant'Anna, S., Teixeira-da-Rocha, M., Grego, K., Travaglia Cardoso, S.R., Moura da Silva, A.M., Fry, B.G., 2018. Coagulotoxicity of *Bothrops* (Lancehead pit-vipers) venoms from Brazil: differential biochemistry and antivenom efficacy resulting from prey-driven venom variation. Toxins 10, 411.
Sutherland, S.K., 1983. Australian Animal Toxins: The Creatures, Their Toxins and Care of the Poisoned Patient. 1983 Oxford University Press, Melbourne, Vic.(Australia).
Tan, N.-H., Tan, C.-S., 1989. The enzymatic activities and lethal toxins of *Trimeresurus wagleri* (speckled pit viper) venom. Toxicon 27, 349–357.
Tan, C.H., Tan, K.Y., Yap, M.K.K., Tan, N.H., 2017. Venomics of *Tropidolaemus wagleri,* the sexually dimorphic temple pit viper: unveiling a deeply conserved atypical toxin arsenal. Sci. Rep. 7, 43237.
Tang, E.L.H., Tan, C.H., Fung, S.Y., Tan, N.H., 2016. Venomics of *Calloselasma rhodostoma*, the Malayan pit viper: a complex toxin arsenal unraveled. J. Proteome 148, 44–56.
Team, R.C., 2016. R: A Language and Environment for Statistical Computing, 3.3, 1 ed. R

Foundation for Statistical Computing, Vienna, Austria.
Trookman, N.S., Rizer, R.L., Ford, R., Ho, E., Gotz, V., 2009. Immediate and long-term clinical benefits of a topical treatment for facial lines and wrinkles. J. Clin. Aesthet. Dermatol. 2, 38.
Vaiyapuri, S., Sunagar, K., Gibbins, J.M., Jackson, T.N.W., Reeks, T., Fry, B.G., 2015. Kallikrein Enzymes, Venomous Reptiles and their Toxins. Oxford University Press, New York.
Wang, R., Kini, R.M., Chung, M.C., 1999. Rhodocetin, a novel platelet aggregation inhibitor from the venom of *Calloselasma rhodostoma* (Malayan pit viper): synergistic and noncovalent interaction between its subunits. Biochemistry 38, 7584–7593.
Warrell, D.A., Looareesuwan, S., Theakston, R.D.G., Phillips, R.E., Chanthavanich, P., Viravan, C., Supanaranond, W., Karbwang, J., Ho, M., Hutton, R.A., 1986. Randomized comparative trial of three monospecific antivenoms for bites by the Malayan pit viper (*Calloselasma rhodostoma*) in southern Thailand: clinical and laboratory correlations. Am. J. Trop. Med. Hyg. 35, 1235–1247.
Weerakkody, R.M., Lokuliyana, P.N., Lanerolle, R.D., 2016. Transient distal renal tubular acidosis following hump nosed viper bite: two cases from Sri Lanka. Saudi J. Kidney Dis. Transplant. 27, 1018.
White, J., 2005. Snake venoms and coagulopathy. Toxicon 45, 951–967.
Williams, D., Gutiérrez, J.M., Harrison, R., Warrell, D.A., White, J., Winkel, K.D., Gopalakrishnakone, P., 2010. The global snake bite initiative: an antidote for snake bite. Lancet 375, 89–91.
Williams, D.J., Gutiérrez, J.-M., Calvete, J.J., Wüster, W., Ratanabanangkoon, K., Paiva, O., Brown, N.I., Casewell, N.R., Harrison, R.A., Rowley, P.D., 2011. Ending the drought: new strategies for improving the flow of affordable, effective antivenoms in Asia and Africa. J. Proteome 74, 1735–1767.
Withana, M., Rodrigo, C., Gnanathasan, A., Gooneratne, L., 2014. Presumptive thrombotic thrombocytopenic purpura following a hump-nosed viper (*Hypnale hypnale*) bite: a case report. J. Venom. Anim. Toxins Incl. Trop. Dis. 20, 26.
Yamada, D., Sekiya, F., Morita, T., 1997. Prothrombin and factor X activator activities in the venoms of Viperidae snakes. Toxicon 35, 1581–1589.
Zulys, V.J., Teasdale, S.J., Michel, E.R., Skala, R.A., Keating, S.E., Viger, J.R., Glynn, M., 1989. Ancrod (Arvin) as an alternative to heparin anticoagulation for cardiopulmonary bypass. Anesthesiology 71, 870–877.